VOL 1, NO.1 (2021) 128-144
https://jagst.utm.my

JAGST
Journal of Advanced Geospatial Science & Technology

Miniature UWB Radar for Accurate Object Detection and Indoor Localisation

Tan Syh Ren[1], Koo Voon Chet[2], Chan Yee Kit[3]
[1, 2, 3]Faculty of Engineering and Technology, Multimedia University, Melaka, Malaysia
Corresponding Email: tsrhelios@gmail.com

Abstract - The demand for precise location has increased throughout the years and is projected to continue to do so in the coming years. However, when it comes to indoor localization applications, satellite-based localisation approaches become more obsolete. Ultra-wideband (UWB) impulse radar is a technology for indoor localization that is model-based. However, the majority of research create the UWB radar's transmitter using discrete components or microwave integrated circuits. On the other hand, receivers are designed independently of the transmitter, with synchronisation between the two essential. In this paper, we present the design of a radar system with X2 Ultra-Wideband (UWB) transceiver system on chip (SoC) as its core. Together with X2, two UWB antennas and LNAs formed the analogue front end of the radar system. A Personal Computer (PC) software developed in VisualBasic.net is used to communicate to a microcontroller which is interfaced with the digital backend of X2. The system demonstrates ranging capability up to 3 meters. The result indicates that the designed UWB impulse radar successfully detected the object with a sufficient error margin. It can be used for a variety of applications, including vehicle counting, vehicle sensor, and human sensor, with appropriate calibration and fine tuning.

Keywords - Ultra-wideband (UWB), *Radar*, *Indoor Localization*

Article History: received 22 December 2020, accepted 6 July 2021, published 1 August 2021

How to cite: Tan, S.R, Koo, V.C. and Chan, Y.K. (2021). Miniature UWB Radar for Accurate Object Detection and Indoor Localisation. Journal of Advanced Geospatial Science & Technology 1(1), 128-144.

1. Introduction

The need for accurate location is growing over the years and is expected to be growing in the upcoming years according to IndustryARC (2017). Satellite based geodetic system such as Global Positioning System (GPS) can be used to provide accurate information for outdoor localisation purpose. Position accuracy of up to 1.368m at 95% of horizontal position error is achievable with GPS stated by William on Hughes Technical Center (2017). Other than GPS, there are some other competing satellites based geodetic systems such as Gallileo, BeiDou and GLONASS which offer similar accuracy (Pan et al., 2016). Data of different constellations can also be integrated to achieve higher accuracy (Pan et al., 2019). However, satellite signal is weaker if there is no line of sight to the satellite. This makes satellite-based localisation techniques become more irrelevant when it comes to indoor localisation applications.

Many types of indoor localization techniques have been discovered. They can be classified into mainly model-based technique and fingerprint technique (Kárník et al., 2016). The time needed for two devices to communicate is proportional with distance between the devices. By placing a mobile device on the interested object and some static devices at known location, the time taken for the mobile device to communicate with the static devices can be translated to actual distance with mathematical model. This is the essential concept of model-based technique (Kárník et al., 2016).

On the other hand, in finger print technique, a database with known sensor reading at known location is built. The sensor is then placed on the object of interest and the sensor reading is continuously updated. The sensor reading will be compared with the database. The distance of the object will be deemed as the distance which has closest sensor reading in the database (Karnik et al., 2016).

Ultra-wideband (UWB) impulse radar is one of the model-based technique. UWB impulse radar emits impulses which have ultra-wideband and measure the time taken for the impulses to return. Federal Communications Commission (FCC) of United States of America defines UWB transmitter bandwidth as equals or greater than 500MHz (Sabath, Mokole, and Samaddar, 2005). The spreading of the Radio Frequency (RF) power over a wide frequency band makes UWB impulses has less interference to signals that have narrow band.

Han et al., (2006), Oh and Wentzloff (2011), Zou, Gupta and Caloz (2017) designed UWB pulse generator with Step Recovery Diode (SRD). Han et al., (2016) drives the SRD with off the shelves operational amplifier and buffer amplifier to achieve higher driving current

of the SRD. The SRD is tuned by varying the delay line which is controlled by mechanical switches. The mechanical switches synthesize different length of trace to short circuit thus producing varying pulse width. Oh and Wentzloff (2011) employs two SRD with one SRD for sharpening of falling edge of input data negative pulse and the other SRD for controlling the pulse width and sharpening of rising edge. Zou, Gupta and Caloz (2017) proposed a pulse generator with a pair of SRD with tunability. By changing a resistor value, the generated pulse width can be changed.

Beev, Keller and Mehlstäubler (2017) and Huang et al., (2014) developed pulse generator with avalanche transistors. Beev, Keller and Mehlstäubler (2017) have developed the pulse generator with commonly available 2N2369 transistor and Field Programmable Gate Array (FPGA) is used for generating the synchronized triggering pulses. Pulse with amplitude of 20V (into 50 Ohm load), 10ns Full Width at Half Maximum (FWHM) and 25 MHz repetition rate is achieved. Li et al., (2015) have analysed the important parameters influencing Gaussian pulse circuit based on Marx circuit-based avalanche transistors. There are 3 main parameters namely charging voltage, charging resistance and charging capacitance. Charging voltage will affect the pulse rise time and amplitude. Charging resistance will influence the maximum pulse repetition rate. Pulse amplitude and fall time will increase when the charging capacitance increases. Huang et al. (2014) have developed a pulse generator with 25 stages Marx band pulse circuit. The pulse generator is able to generate pulses with significantly higher amplitude (2.7 kV into 50 Ohm load) and lower FWHM (1 ns) but the repetition rate is limited to 10 kHz.

Zhang, Fathy and Mahfouz (2007); Malajner, Šipoš and Gleich (2020) implemented UWB receiver with Equivalent Sample Time (EST) samplers with discrete components such as balun, schottky diode and etc. to avoid the use of expensive high-speed ADC. Han and Nguyen (2006) developed a tunable multiband UWB radar sensor using multiple microwave integrated circuit. The transmitter and receiver are fabricated on two different Printed Circuit Board (PCB) which house the discrete components and microwave integrated circuits. Kulmer et al., (2017) has developed an indoor positioning system with DecaWave's DW1000 UWB transceiver. DW1000 is IEEE 802.15.4 compliant. It relies on the measurement of communication time between two DW1000 which function as tag and anchor. Accuracy of 0.5m has been achieved. Besides DW1000, Ruiz and Granja (2017) have investigated the performance of other UWB localisation solution such as BeSpoon's SpoonPhone and Ubisense's Ubisense 7000 but their accuracy is inferior to DW1000.

The works done by most of the groups above are constructing the transmitter of the UWB radar from discrete components or microwave integrated circuits. On the other hand, the receivers are constructed separately with synchronization required between transmitter and receiver. For the solution with DW1000 Integrated Circuit (IC), at least two ICs are required (to function as tag and anchor) to implement the solution.

In this paper, we present a design of UWB impulse radar with X2 SoC as the core of the radar (Novelda, 2015). The use of a single SoC to construct the UWB radar instead of using discrete components eliminates the uncertainty of the radar system due to the process variation of the individual components. The minimum amount of IC required to implement the solution is only one X2 compared to DW1000, Ubisense 7000 or SpoonPhone which require at least two ICs.

X2 has UWB impulse transceiver, timing delay measurement unit, coherent integrator or received signal amplitude as well as digital communication and control via Serial Peripheral Interface (SPI). The RF input and output of the transceiver is single ended instead of differential. These features make it a PCB area saving solution. A microcontroller can be used to control the SoC to perform the desired operations such as initialization of the SoC, generation of UWB impulses, UWB impulses amplitude measurement, measurement of time delay between transmission and receiving of UWB impulses as well as the dumping of memory that contains the received radar frame amplitude. Software that is developed with VisualBasic.net to run on a PC is retrieving the radar frames continuously from the microcontroller and performs the processing power consuming tasks such as data processing algorithm and data visualization to determine the distance of an object to the radar.

2. System hardware

The system consists of mainly four blocks: PC, microcontroller, X2 SoC breakout board (UWB transceiver module) and analog frontend. Figure 1 shows the interaction between all blocks in the system.

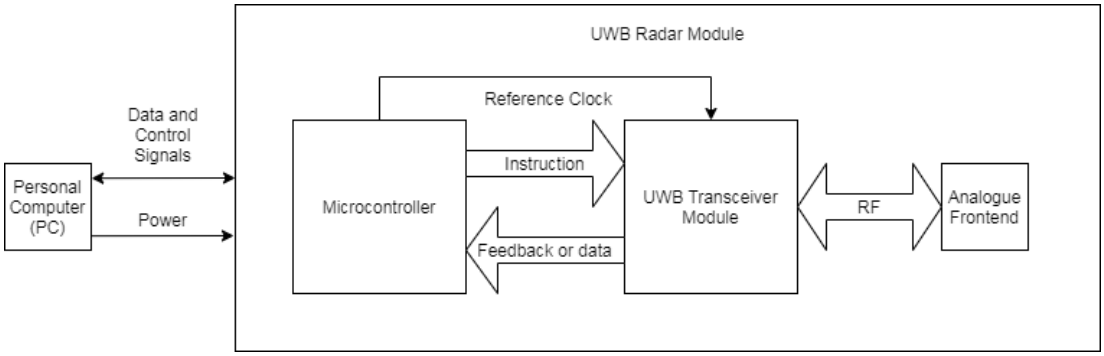

Figure 1. Block Diagram of UWB Impulse Radar

The PC is at the highest hierarchy in the system. Its function is to give instructions to the microcontroller and retrieve received radar frame from the microcontroller via virtual communication (COM) port. Besides that, it also supplies the power to all low-level hardware via Universal Serial Bus (USB) power supply.

Figure 2 shows the essential hardware blocks of the microcontroller platform. The microcontroller platform is able to configure, control and read data from X2 SoC via SPI port. Besides that, the microcontroller platform delivers the UWB 5V supply it receives from the PC to the X2 SoC breakout board. Upon powering up, the microcontroller provides a 16 MHz clock to X2 SoC and also initializes it. After that, the microcontroller waits for the command from PC via the virtual COM port.

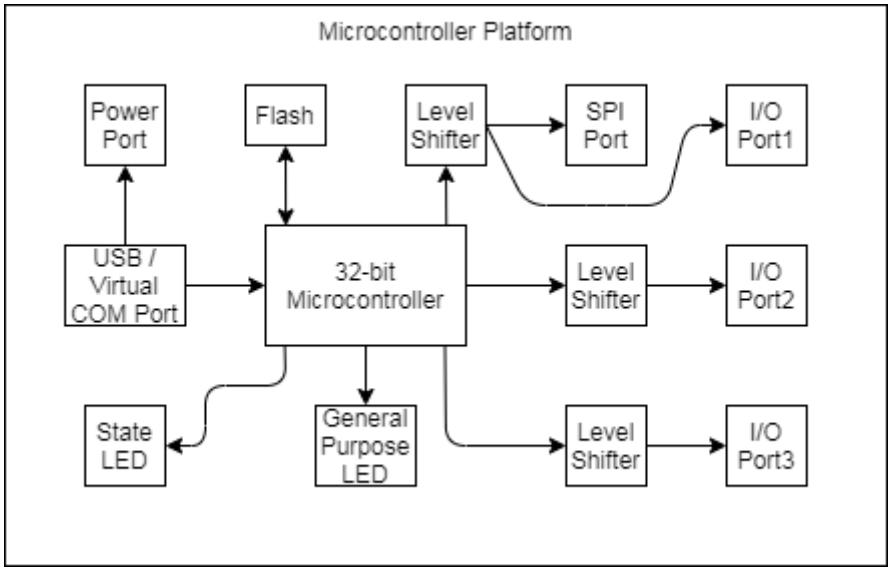

Figure 2. Microcontroller Platform's Block Diagram

X2 SoC is the core of the radar. Upon receiving the SPI command, it will transmit UWB impulses and also translate the received radar frame amplitude into 255 32-bit integer values. The radar frame can be read by the microcontroller via SPI. There is also on chip time measurement unit that is able to measure the sampling period of the radar frame as well as the delay between transmitter and receiver. The time offset between transmitter and receiver triggering is configurable. This makes X2 able to measure objects placed at different ranges that exceeds the total sampling period of single radar frame.

Figure 3 shows the block diagram of the breakout board of X2 SoC. X2 SoC is soldered onto a breakout board which besides housing X2 also provides necessary operation conditions for X2 such as 2.5V and 1.5V voltage supply and 10uA reference current. 2.5V and 1.5V supplies are generated from 5V supplied by USB power. LT3092 current regulator has a SET pin that provides 10 uA set current and OUT pin to provide the higher current needed in the application (Analog Devices, 2018). 10uA reference current is generated from the set current of the current regulator LT3092 for X2. Last but not least, it interfaces header pins and SubMiniature version A (SMA) connectors to the digital and RF pins of X2.

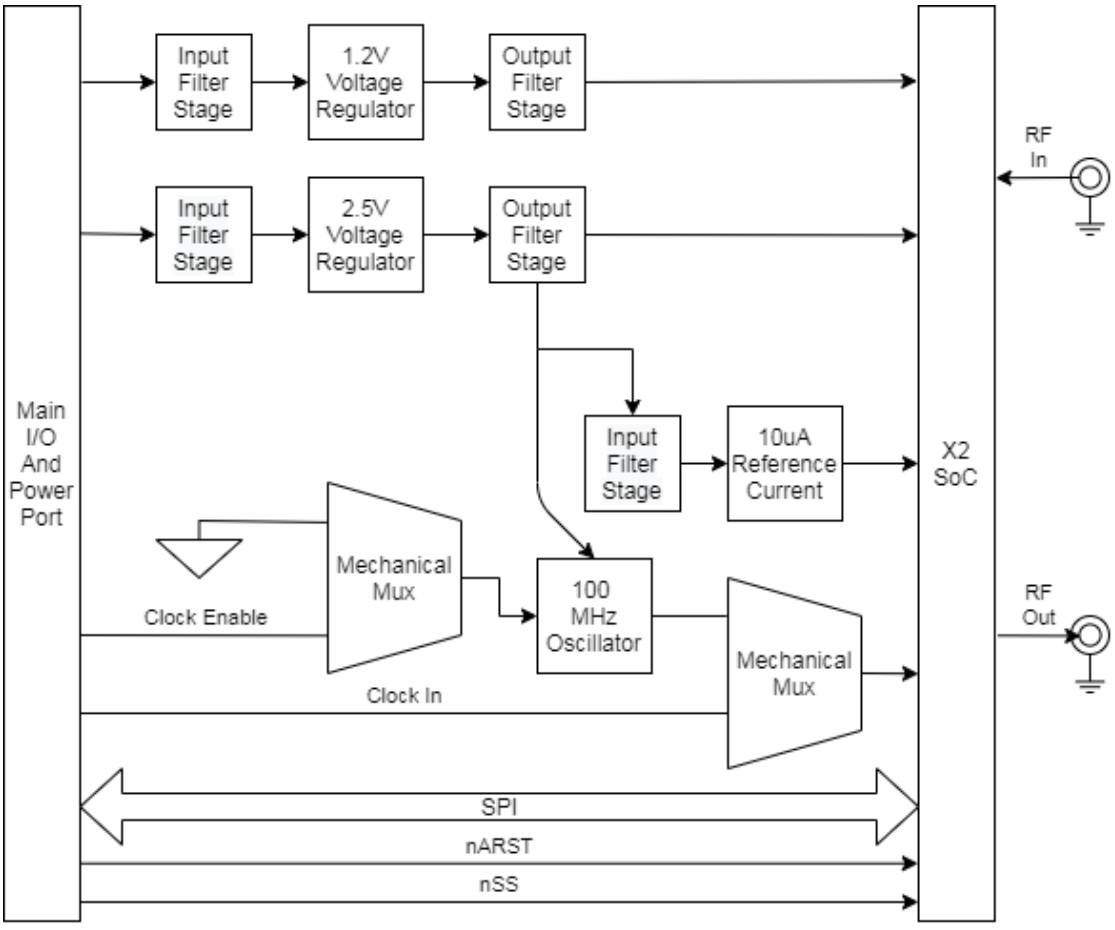

Figure 2. Block Diagram of X2 SoC Breakout Board

The analogue front end provides the possibility for X2 to transmit and receive RF power. Figure 4 shows the block diagram of the analogue frontend. The RF input and output of X2 are connected to the analog front end which consists of a low noise amplifier, a UWB antenna and a Direct Current (DC) block for each RF input and output. The Low Noise Amplifiers (LNAs) serve to improve the Signal to Noise Ratio (SNR) of the impulse radar while the antennas radiates and capture and UWB impulses. DC block is necessary to filter out the common mode component of the received radar frame. Without the DC block the received radar frame will observe common mode fluctuation.

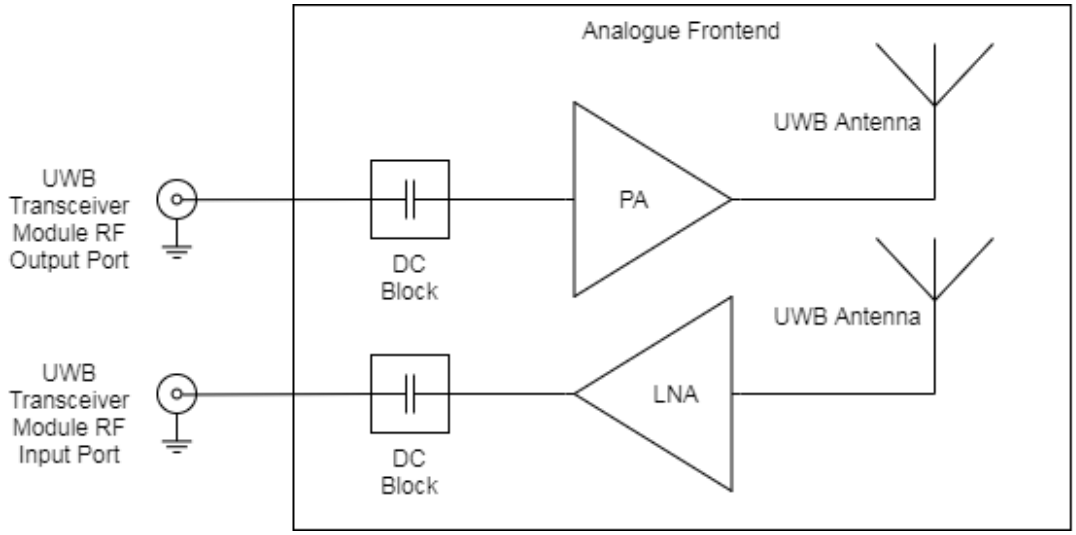

Figure 3. Block Diagram of Analogue Frontend

3. Methodology

There are 2 main functions in the radar to perform ranging: measurement of the time delay between transmitted and received radar frame to calculate the distance of the object from the radar and process the data frame to determine whether an object is present in the radar frame

The mathematical model that radars relies on is the electromagnetic wave propagation speed in empty space. This is applicable for UWB impulse radar too. The mathematic equation and describe the time delay of the impulse radar is described in equation (1), where d is the distance travelled by the electromagnetic wave, v is the propagation velocity of electromagnetic wave in air which is the approximately equals to speed of light and t is the time delay between transmission and receiving of the electromagnetic wave (Wolff).

$$d = \frac{vt}{2} \qquad (1)$$

However, equation (1) is an ideal equation that models the round trip of electromagnetic wave without considering the practicality of a radar system. To correctly model the UWB impulse radar distance measurement, equation (1) is modified into equation (2) to consider the intrinsic delay time induced by the radar system components such as connectors, wiring and etc. which is denoted as T_o.

$$d = \frac{v(t - T_o)}{2} \qquad (2)$$

Since T_o is fixed and can be found empirically, t becomes the only variable needed to be measured. The delay between triggering of the transmission and receiving of UWB impulses, t_d, is configurable and measurable in X2 (Novelda, 2015). The sampling period of 255 data points of the captured radar frame is also measurable (Novelda, 2015). The time delay of each data point from start of frame can be estimated as sampling period, T_s, of the whole radar frame divided by sample size, N, which is 255 (Novelda, 2015).

With t_d, T_s, and N known, the time delay of nth data point in the received radar frame can be calculated with equation (3).

$$t_n = t_d + \frac{T_s \times n}{N} \qquad (3)$$

By replacing the t in equation (2) with equation (3), the distance represented by the amplitude of each of the 255 data points of the radar frame, d_n, can be calculated with equation (4).

$$d_n = \frac{v(t_d + \frac{T_s \times n}{N} - T_o)}{2} \qquad (4)$$

With the distance represented by each data point in the radar frame known, it is insufficient to perform ranging function for the UWB impulse radar. The radar frame has to be processed in order to determine whether an object is present algorithmically. The algorithm developed for the UWB impulse radar can be summarized in 8 steps.

1. Discover the values of the settings required to configure t_d to cover the desired measurement range. If a single radar frame cannot cover the whole range, multiple sets of settings will be determined in order to cover the whole desired range with multiple radar frame measurement.
2. After the amount of radar frames required to cover the desired range and the settings to configure the t_d of each radar frame are determined, initial measurement of each radar frame will be made to serve as the reference baseline for subsequent measurements.
3. After the reference baseline is established, the radar starts to measure the amplitude of the radar frames. The measured radar frames will subtract the baseline to identify the change of amplitude.
4. After all the radar frames that are required to cover the whole desired range are measured, they are concatenated into a single continuous radar frame.
5. The single radar frame is processed with moving average filter to filter out the noise present in the data.
6. After the amplitude of the radar has been passed through the moving average filter which is a low pass filter, an object is deemed to be present at a particular data point in the radar frame if the amplitude of the radar frame fulfils two criteria: the amplitude of the data point is a local maxima and the amplitude is higher than certain threshold.
7. If there is no presence of object in the radar frame, the reference baseline is updated with the latest measurement. Else, the reference baseline is not updated.
8. Repeat step 3 to 7.

X2 is able to configure t_d by varying the SampleDelay Coarse Tune (SDCT) and SampleDelay Medium Tune (SDMT) registers. Different combination of SDCT and SDMT will result in different t_d. If more than one radar frame is required to cover the desired measurement range, the subsequent nth radar frame would have its t_d equals to (n-1) the radar frame's $t_d + T_s$ as described in equation (5).

$$t_{d(n)} = t_{d(n-1)} + T_s \qquad (5)$$

By varying SDCT and SDMT different t_d will be configured for different radar frames to cover different measurement ranges. After the setting of SDCT and SDMT for all radar frames are determined, each radar frames are measured for 30 times and placed in a circular buffer which is a First in First Out (FIFO) memory. The FIFO memory has the size of 28 frames, so a total of 840 radar frames are measured during initialization to fill up the circular buffer. Reference baseline radar frames will be generated as the average of the 28 radar frames in the circular buffer.

Using the average of 28 samples instead of 1 sample as the reference baseline gives a low pass filter ability for the radar. Since the scanning frequency of the UWB impulse radar is configured to be 4 Hz, the reference baseline will essentially be generated from the measurements of past 7 seconds. This makes the reference baseline generated able to serve to distinguish between the static environment measurements and the measurements that have detected objects but at the same time able to include the slowly changing environmental factors such as change of measurement amplitude or change of noise floor due to the change of temperature and etc.

After the reference baseline has been established, the UWB impulse radar will start to continuously retrieve the readings of each radar frame. Each radar frame will be subtracted with the reference baseline and the absolute value of the amplitude in term of millivolt will be considered as the "real" amplitude of the radar frames. This step will highlight the change of amplitude compared to the reference baseline which might indicate the presence of an object.

After all the radar frames required to cover the whole desired measurement range are collected, they are concatenated to form a single continuous radar frame. A moving average filter which is a digital low pass filter is applied to the single radar frame to filter out high frequency noise. Then, each of the data point in the single radar frame is analysed for the presence of an object. There are two decision criteria for the presence of an object at a particular data point: the data point is a local maxima and it is above the defined threshold.

The criterion of local maxima is that the data point should be greater than the 10 data points before and 10 data points after it. The threshold of object presence is defined by a decay function in equation (6). In the decay function, it is important that n should be a negative value

so the exponential term will be decreasing. As n is negative, k will be the final value of the function when d, the distance measured by the radar is approaching infinity. The term r is used to scale and control the rolloff of the exponential term. After some trial and error, the constants are set as k = 1.3, n = -2 and r = 10. This will produce a decay function as shown in Figure 5. If a data point is a local maxima in the radar frame and its amplitude is higher than the decay function, it is considered to represent an object.

$$Threshold = k + e^{(n \times d)} \times r \quad (6)$$

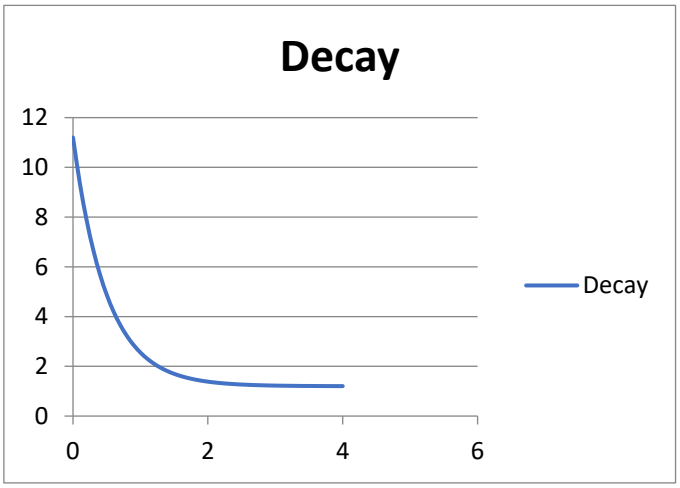

Figure 4. Decay function with k = 1.3, n = -2 and r = 10

4. Experiments and results

Two experiments were done separately in indoor environment and open field. The experiment setups as shown in Figure 6 consist of the UWB impulse radar module, a PC to run the radar processing program, a measuring tape as reference, a metal box as the artificial point target to be detected and an Android phone to be used as the remote control of the radar.

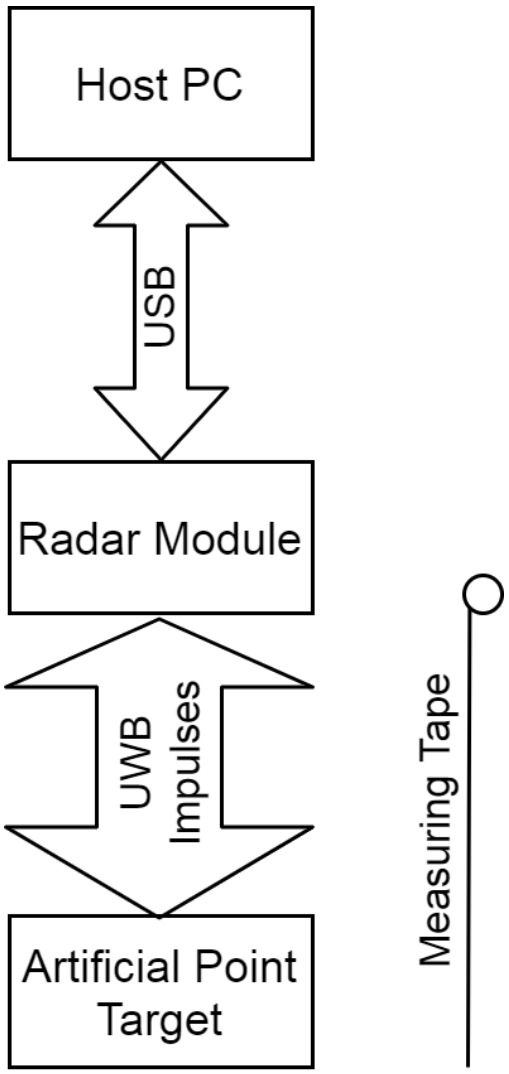

Figure 5. Experiment Setup

The setups are calibrated differently as well as the sensitivity (*k* term of the decay function) are adjusted to cope with the behaviour of the radar in different environment. In indoor environment, the UWB impulse radar module was placed on a chair while another chair were placed in front of the radar at approximate location of the intended measurement distance. After the environment was measured by the radar, the artificial point target (metal box) was placed on the chair.

The setups are calibrated differently as well as the sensitivity (*k* term of the detection threshold decay function) are adjusted to cope with the behaviour of the radar in different environment. The calibration was focused on eliminating the intrinsic RF delay within the system and the adjustment of the tilting angle of the RF module to face the object in front with right angle for both horizontal and vertical direction.

For the simulated indoor environment, the UWB impulse radar module was placed on a chair while another chair was placed in front of the radar at approximate location of the intended measurement distance. The chairs are placed near a sofa to consider the effect of furniture in indoor environment. After the environment was measured by the radar, the metal box was placed on empty chair as illustrated in Figure 7.

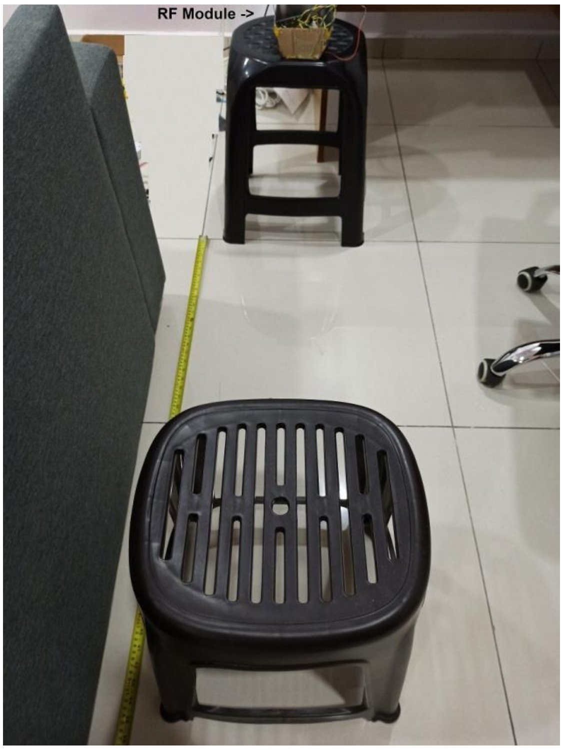

Figure 6. Indoor Measurement Setup

The distance to the first detected object reported by the radar was taken as the measured distance by the radar. The result is shown in Table 1.

Table 1. Indoor Measurement Result

Measuring Tape (m)	Radar (m)	Error (m)
1	1.0085	0.0085
2	1.9745	-0.0255
3	2.9762	-0.0238

In open field environment, the same hardware was setup accordingly. The difference of the open field and simulated indoor environment is that there was significantly less object compared to indoor simulation as illustrated in Figure 8. The result is shown in Table 2.

Figure 7. Open Field Environment

Table 2. Open Field Measurement Result

Measuring Tape (m)	Radar (m)	Error (m)
1	1.0083	0.0084
2	1.9628	-0.0371
3	3.0080	0.0080

5. Conclusion

The result shows that the UWB impulse radar developed successfully detected the object with adequate error margin. The radar can be further miniaturized by doing full custom design on all the hardware used to reach the full potential of miniaturization of this design. The bulky hardware used such as the DC blocks, LNAs and antennas can be substituted with capacitors, solid state LNAs and PCB layout antenna. Other than that, the microcontroller which is an off

the shelve Arduino can be replaced with a custom design to exclude the unnecessary features come with an Arduino for compatibility purpose such as the pinout and form factor. In this way, it is possible to integrate the microcontroller and the RF components together into one single PCB or two PCBs with stacking configuration.

Calibration of the UWB impulse radar is crucial for it to report accurate distance which is common for modern electronic measurement system. The UWB impulse radar is very sensitive to the change of the state of the hardware or environment. Thus, whenever the RF module has been moved, recalibration is required in order for the radar to report accurate result. Calibration of zeroth order effect (intrinsic delay of the RF power within the system) is crucial as the movement of the wiring or any slight change of the dimension of the hardware will affect this parameter. Besides that, elevation angle of the RF module and the metal box will also influence the result. Thus, the difference of elevation angle of the RF module and the metal box should be made as small as possible.

Other than that, the environment should be as static as possible in order to easily distinguish the reported distance measurement caused by the measurement object versus the reported distance caused by the movement of another object, if any. For indoor environment, the *k* term of the sensitivity has been set to 1.3mV while for the open field it was set to 3mV. This is due to the increased noise in the open field compared to indoor environment. In order to avoid false positive for distanced object (>1m), raising the sensitivity threshold is necessary.

Both indoor and open field measurements have shown similar measurement and error. However, there is less reflection at open filed environment compared to indoor environment. The theoretical resolution of the system is directly related to the sampling delay of each of the 255 data point. The sampling period obtained by experiment is around 0.025ns which is equivalent to 0.00375m by assuming the RF signal is travelling at speed of light. However, the sampling period is not guaranteed by design of X2 and is subject to change with environment. This contributes to the uncertainty of the measurements.

Besides sampling period, there are other error sources that contribute to the uncertainty of the measurement such as parallax error when reading the measuring tape, the accuracy of the calibration and post processing of the raw data. The raw data is passed through average filter which will distort the raw data to a certain degree. Therefore, we concluded that with adequate calibration and fine tuning, it can be implemented for some applications such as vehicle counting, vehicle sensor or human sensor.

Acknowledgment

The authors would like to thank the Multimedia University for supporting this study. Also, we appreciate the comments of the anonymous reviewers in revising the paper.

References

Analog Devices. "LT3092 Datasheet and Product Info." Analog Devices. August 2018. https://www.analog.com/media/en/technical-documentation/data-sheets/lt3092.pdf.

Beev, N., Keller, J. and Mehlstäubler, T.E., 2017. *"Note: An Avalanche Transistor-Based Nanosecond Pulse Generator with 25 MHz Repetition Rate"*. Review of Scientific Instruments, 88(12), :126105.

Han, J. and Nguyen, C., 2006. *"On the Development of a Compact Sub-Nanosecond Tunable Monocycle Pulse Transmitter for UWB Applications"*. IEEE Transactions on Microwave Theory and Techniques, 54(1), :285-293.

Han, J. and Nguyen, C., 2006. *"Development of a Tunable Multiband UWB Radar Sensor and Its Applications to Subsurface Sensing"*. IEEE Sensors Journal, 7(1), :51-58.

Huang, Z., Fu, Q., Chen, P., Yang, H. and Yang, X., 2014, December. *"High Power Pulse Generator Based on Avalanche Transistor Marx Circuit"*. In 2014 IEEE International Conference on Communiction Problem-Solving (:315-317). IEEE.

IndustryARC. "Indoor Positioning and Navigation Market - Forecast (2021 - 2026)." Market Forecast Report, 2017.

Kárník, J. and Streit, J., 2016. *"Summary of Available Indoor Location Techniques"*. IFAC-PapersOnLine, 49(25), :311-317.

Kulmer, J., Hinteregger, S., Großwindhager, B., Rath, M., Bakr, M.S., Leitinger, E. and Witrisal, K., 2017, May. *"Using Decawave UWB Transceivers for High-Accuracy Multipath-Assisted Indoor Positioning"*. In 2017 IEEE International Conference on Communications Workshops (ICC Workshops), :1239-1245, IEEE.

Malajner, M., Šipoš, D. and Gleich, D., 2020. *"Design of a Low-Cost Ultra-Wide-Band Radar Platform"*. Sensors, 20(10), :2867.

Novelda. "X2 Datasheet." Laonuri Web Site. Oct 1, 2015. http://laonuri.techyneeti.com/wp content/uploads/2019/02/X2_DATASHEET.pdf.

Oh, S. and Wentzloff, D.D., 2011, September. *"A Step Recovery Diode Based UWB Transmitter for Low-Cost Impulse Generation"*. In 2011 IEEE International Conference on Ultra-Wideband (ICUWB) (:63-67). IEEE.

Pan, L., Cai, C., Santerre, R. and Zhang, X., 2017. *"Performance Evaluation of Single-Frequency Point Positioning with GPS, GLONASS, Beidou and Galileo"*. Survey Review, 49(354), :197-205.

Pan, L., Zhang, X., Li, X., Li, X., Lu, C., Liu, J. and Wang, Q., 2019. *"Satellite Availability and Point Positioning Accuracy Evaluation on a Global Scale for Integration of GPS, GLONASS, Beidou and Galileo"*. Advances in Space Research, 63(9), :2696-2710.

Ruiz, A.R.J. and Granja, F.S., 2017. *"Comparing Ubisense, Bespoon, and Decawave UWB Location Systems: Indoor Performance Analysis"*. IEEE Transactions on Instrumentation and Measurement, 66(8), :2106-2117.

Sabath, F., Mokole, E.L. and Samaddar, S.N., 2005. *"Definition and Classification of Ultra-Wideband Signals and Devices"*. URSI Radio Science Bulletin, 2005(313), :12-26.

Team, G.P., 2014. *"Global Positioning System (gps) Standard Positioning Service (sps) Performance Analysis Report"*. GPS Product Team: Washington, DC, USA.

Wolff, Christian. Radar Basics - Range or distance measurement. n.d. https://www.radartutorial.eu/01.basics/Distance-determination.en.html (accessed June 14, 2021).

Zhang, C., Fathy, A.E. and Mahfouz, M., 2007. *"Performance Enhancement of a Sub-Sampling Circuit for Ultra-Wideband Signal Processing"*. IEEE Microwave and Wireless Components Letters, 17(12), :873-875.

Zou, L., Gupta, S. and Caloz, C., 2017. *"A Simple Picosecond Pulse Generator Based on a Pair of Step Recovery Diodes"*. IEEE Microwave and Wireless Components Letters, 27(5), :467-469.